



HAL
open science

On-line enrichment of N-glycans by immobilized metal-affinity monolith for capillary electrophoresis analysis

Huikai Shao, Balazs Reider, Gabor Jarvas, Andras Guttman, Zhengjin Jiang,
N. Thuy Tran, Myriam Taverna

► To cite this version:

Huikai Shao, Balazs Reider, Gabor Jarvas, Andras Guttman, Zhengjin Jiang, et al.. On-line enrichment of N-glycans by immobilized metal-affinity monolith for capillary electrophoresis analysis. *Analytica Chimica Acta*, 2020, 1134, pp.1 - 9. 10.1016/j.aca.2020.08.002 . hal-03491245

HAL Id: hal-03491245

<https://hal.science/hal-03491245>

Submitted on 24 Aug 2022

HAL is a multi-disciplinary open access archive for the deposit and dissemination of scientific research documents, whether they are published or not. The documents may come from teaching and research institutions in France or abroad, or from public or private research centers.

L'archive ouverte pluridisciplinaire **HAL**, est destinée au dépôt et à la diffusion de documents scientifiques de niveau recherche, publiés ou non, émanant des établissements d'enseignement et de recherche français ou étrangers, des laboratoires publics ou privés.



Distributed under a Creative Commons Attribution - NonCommercial 4.0 International License

1 **On-line enrichment of N-glycans by immobilized metal-affinity**
2 **monolith for capillary electrophoresis analysis**

3
4 Huikai Shao^{a,b,*}, Balazs Reider^{c,*}, Gabor Jarvas^{c,d}, Andras Guttman^{c,d}, Zhengjin Jiang
5 ^{b**, N Thuy Tran^{a**, Myriam Taverna^{a,e}}}

6
7 ^a Université Paris-Saclay, CNRS, Institut Galien Paris Saclay, 92296, Châtenay-
8 Malabry, France.

9 ^b Institute of Pharmaceutical Analysis, College of Pharmacy, Jinan University,
10 Guangzhou, 510632, China

11 ^c Translational Glycomics Research Group, Research Institute of Biomolecular and
12 Chemical Engineering, University of Pannonia, 10 Egyetem Street, Veszprem 8200,
13 Hungary

14 ^d Horváth Csaba Memorial Laboratory of Bioseparation Sciences, Research Centre for
15 Molecular Medicine, Faculty of Medicine, University of Debrecen, 98 Nagyerdei Krt,
16 Debrecen 4032, Hungary

17 ^e Institut Universitaire de France (IUF)

18

19 * Both first authors contributed equally to this manuscript.

20 ** Corresponding authors

21 Nguyet Thuy Tran thuy.tran-maignan@universite-paris-saclay.fr

22 Zhengjin Jiang jzjjackson@hotmail.com

23

24

25 **List of Abbreviations:**

26 ACN, acetonitrile; AIBN, 2, 2-azobisisobutyronitrile; AM, acrylamide; APTS, 1-
27 aminopyrene-3, 6, 8-trisulfonic acid; BAA, bis-acrylamide; CE, capillary
28 electrophoresis; DMF, N, N'-dimethylformamide; DMSO, dimethylsulfoxide; EGMP,
29 ethylene glycol methacrylate phosphate; ESI, electrospray ionization; GU: Glucose
30 units; HCl, Hydrochloric acid; IMAC, immobilized metal-affinity chromatography; LC,
31 liquid chromatography; LIF, laser induced fluorescence; LiOH, lithium hydroxide
32 monohydrate; MALDI, Matrix assisted laser desorption ionization; Man, Mannose;
33 MeOH, methanol; MIP, mercury intrusion porosimetry; MS, mass spectrometry; NaOH,
34 Sodium hydroxide; PGC, Porous graphitized carbon; PNGase F, Peptide N-
35 Glycosidase F; RNase B, Ribonuclease B; SEF, Signal enrichment factor; SEM,
36 scanning electron microscopy; SPE, Solid phase extraction; THF, tetrahydrofuran; UV,
37 ultraviolet; $ZrOCl_2 \cdot 8H_2O$, Zirconium dichloride oxide hydrate; γ -MAPS, γ -
38 methacryloxypropyltrimethoxysilane.

39

40 **Abstract:**

41 A novel N-glycan enrichment strategy is presented using unexpected but strong
42 interactions between the sulfonate groups brought by the fluorescent dye of glycans and
43 the Zr^{4+} modified poly(ethylene glycol methacrylate phosphate (EGMP)-*co*-acrylamide
44 (AM)-*co*-bis-acrylamide (BAA)) monolith. The poly (EGMP-*co*-AM-*co*-BAA)
45 monolith was synthesized *via* ultraviolet (UV) irradiation and then functionalized with
46 Zr^{4+} . The obtained monolith was characterized with scanning electron microscopy and
47 mercury intrusion porosimetry. Large through-pores and a continuous skeleton with
48 high permeability were observed. The N-glycans were labeled with the 1-aminopyrene-
49 3, 6, 8-trisulfonic acid (APTS) and enriched by the Zr^{4+} modified monolith through
50 IMAC interaction. This enrichment step was then coupled off-line to capillary
51 electrophoresis (CE) separation with laser induced fluorescence (LIF) detection.
52 Successful preconcentration of the APTS labeled maltooligosaccharide ladder was
53 achieved under optimized conditions. Enrichment factors obtained for the
54 maltooligosaccharides ranged from 9 to 24 with RSDs from 2.0% to 9.2% (n = 3).
55 Moreover, very good repeatabilities (< 6.7%) were obtained for glucose oligomers (4
56 to 15 glucose units) corresponding to sizes expected for N-glycans, demonstrating the
57 great potential of this Zr^{4+} modified monolith to enrich APTS labeled glycans from N-
58 glycoproteins. The proposed method was then successfully applied for the enrichment
59 of N-glycans released from Ribonuclease B, in which case all five expected
60 oligomannose glycans (Man 5 to Man 9) were successfully enriched. Thanks to the
61 advantage of the method to enrich selectively APTS-glycans compared to the

62 commercial SPE columns composed of HILIC or PGC materials, the first proof of
63 concept of on-line enrichment coupled to CE-LIF separation was demonstrated for
64 maltooligosaccharides as well.

65

66 **Keywords:** N-glycan, zirconium phosphate monolith, solid support, IMAC
67 preconcentration, capillary electrophoresis.

68

69

70 **1 Introduction**

71 As a prevalent post-translational modification of proteins, N-glycosylation plays a
72 key role in a wide range of physiological and pathological processes, such as cell
73 growth, adhesion, cell-cell recognition and signal transduction, [1-3]. N-glycan chains
74 of glycoproteins are essential to their folding, stability, solubility and biological activity.
75 Altered N-glycosylation is reportedly associated with several diseases such as
76 congenital disorders of glycosylation (CDGs) [4], Alzheimer's disease [5] or cancers
77 [6]. N-glycosylation analysis of specific proteins present in biological samples has
78 already allowed the identification of powerful and reliable biomarkers of several
79 diseases like type 2 diabetes [7], hepatic cirrhosis [8], ovarian cancer [9]. Currently,
80 glycan profiling represents one of the best ways to evaluate asparagine linked
81 glycosylation profiles and to detect even minor changes.

82 In general, N-glycans are released from glycoproteins using an enzymatic digestion
83 (e.g., PNGase F) or a chemical reaction (e.g., NaOCl). The main analytical techniques
84 to map released N-glycans are high performance liquid chromatography (LC) [10],
85 capillary electrophoresis (CE) [11], mass spectrometry (MS) [12] or LC-MS [13] and
86 CE-MS [14-15]. However, due to the low abundance of some plasma glycoproteins,
87 the lack of chromophore or fluorophore groups in carbohydrates and their poor
88 ionization efficiency in ESI or MALDI MS, glycan derivatization is highly desirable to
89 enhance their detection sensitivity with all of these techniques. Three labeling sites are
90 available for covalent derivatization in N-glycans: the reducing terminal (-CHO, -NH₂),
91 hydroxyl groups and the carboxyl groups of sialic acids. Although derivatization

92 increases sensitivity, it is often also necessary to enrich N-glycans before their analysis.
93 Most commonly used enrichment methods are based on solid phase extraction (SPE)
94 [15-16] with porous graphitized carbon (PGC) [17-18] or hydrophilic supports [19].
95 However, these chromatographic supports exhibit quite low selectivities. More specific
96 sorbents like lectins- [20], boronate- [21], hydrazine-based materials [22] or those
97 relying on lanthanides [23] have also been described as interesting alternatives for N-
98 glycan enrichment, most frequently before derivatization. Recently, however, a few
99 groups reported strategies involving enrichment after derivatization and relying on the
100 interaction between the derivatization agent attached to the glycans and the solid
101 support [24-25]. Although monolithic columns have attracted great interest in the last
102 decades for sample enrichment due to their flexible synthesis, adjustable porosity, fast
103 mass transport, and tunable surface chemistry [26], they have been mostly used for the
104 enrichment of glycopeptides or intact glycoproteins [27], except one work that focused
105 on non-derivatized glycans derived from glycoproteins [28]. In that work, the monolith
106 was composed of glycidyl methacrylate and ethyleneglycol dimethacrylate and
107 functionalized with cobalt phthalocyanine tetracarboxylic acid (CoPcTc) and glycans
108 were captured via the formation of hydrogen bonds with nitrogen groups in isoindole
109 subunits of CoPcTc. Until now and to the best of our knowledge, no paper has yet
110 reported the possibility to enrich derivatized glycans released from glycoproteins using
111 monolith, the main supports being magnetic mesoporous silica composite [29], silica
112 gel [30] and cotton wool [31].

113 In addition, only one work described immobilized metal affinity chromatography

114 (IMAC) based method for the enrichment of derivatized N-glycans [24]. In that work,
115 the carbohydrates were labeled with a 4-aminophenylphosphate that allowed them to
116 strongly adsorb on Ti^{4+} -microspheres. Excellent selectivity, high enrichment recovery
117 (90%) but poor reproducibility (15%) have been obtained. However, this protocol was
118 based on a new dye that had been exploited only for MALDI-MS analyses of glycans.

119 CE coupled to laser induced fluorescence (LIF) is a powerful separation technique
120 to map N-glycans. Most of the time they are derivatized with 8-aminopyrene-1,3,6-
121 trisulfonic acid (APTS) and glycan isomers can be separated with quite high
122 repeatabilities and resolutions [32-33]. In addition, silica capillaries are well suited for
123 in-situ synthesis of monoliths.

124 This prompted us to develop a capillary monolith-based enrichment of APTS-labeled
125 N-glycans compatible with an on-line coupling to their CE-LIF analysis. The
126 advantageous feature of the IMAC-based enrichment selected in this paper over our
127 previous work on phosphopeptide enrichment in microchips [34] is based on the
128 interaction between the sulfonate groups brought by the APTS and the Zr^{4+} ions
129 immobilized on the monolith, not yet exploited, making it more selective to APTS-
130 glycans compared to commercial SPE columns composed of PGC or HILIC materials.
131 For this purpose, the synthesis of a poly(ethylene glycol methacrylate phosphate
132 (EGMP)-*co*-acrylamide (AM)-*co*-bis-acrylamide (BAA))-based monolith with
133 phosphate groups and immobilized Zr^{4+} was first optimized in the capillary and then
134 characterized in terms of porosity, permeability and mechanical resistance too. The free
135 APTS dye and APTS labeled maltooligosaccharide ladder were employed for

136 optimizing the enrichment procedure and the off-line CE-LIF was used to measure the
137 enrichment efficiency. The developed method was applied for the enrichment and
138 detection of the N-glycans of Ribonuclease B. Finally, the first proof of concept of on-
139 line enrichment coupled to CE-LIF separation was demonstrated for APTS-
140 maltooligosaccharides.

141

142 **2 Materials and Methods**

143 **2.1 Materials**

144 Ethylene glycol methacrylate phosphate (EGMP) was purchased from ESSCHEM
145 (Europe Seaham, United Kingdom). γ -methacryloxypropyltrimethoxysilane (γ -MAPS),
146 acrylamide : bisacrylamide (AM : BAA, mixture ratio 19:1), dimethylsulfoxide
147 (DMSO), 1-dodecanol, N, N'-dimethylformamide (DMF), 2, 2-azobisisobutyronitrile
148 (AIBN), zirconium dichloride oxide hydrate ($ZrOCl_2 \cdot 8H_2O$, > 95%), formic acid (>
149 99%), lithium hydroxide (LiOH) monohydrate, lithium acetate dihydrate (LiAc), acetic
150 acid (> 99%), ammonium hydroxide (28%), 1 M sodium cyanoborohydride/THF,
151 PNGase F enzyme, $NaBH_3CN$, ribonuclease B (RNase B) and PTFE fluid tube (OD:
152 1.8 mm, ID: 0.3 mm) were bought from Sigma-Aldrich (St Louis, MO, USA). 1 M
153 sodium hydroxide (NaOH) and 1 M hydrochloric acid (HCl) solutions, tetrahydrofuran
154 (THF), acetone, methanol (MeOH) and acetonitrile (ACN) were obtained from VWR
155 International (Paris, France). The fast glycan labeling and analysis kit, including the
156 tagging dye of 8-aminopyrene-1,3,6-trisulfonic acid (APTS) and magnetic beads for
157 excess dye removal were from SCIEX (Brea, CA, USA). All water used in the

158 experiments was purified with a Milli-Q system from Millipore (Direct-Q 3, Merck
159 Millipore, Darmstadt, Germany). UV-transparent (TSH) and polyimide capillary
160 columns with 50 μm I.D. were from Polymicro technologies (Phoenix AZ, United
161 States).

162

163 **2.2 Instrumentation**

164 A Bio-link BLX-E365 UV oven (Vilbert Lourmat, Marne La Vallée, France) was
165 used for the photopolymerization for synthesizing the poly(EGMP-*co*-AM-*co*-BAA)
166 monolith. Permeability of the poly(EGMP-*co*-AM-*co*-BAA) monolith was measured
167 using the G2226A nano pump (Agilent Technologies, Santa Clara, USA). Morphology
168 of the poly(EGMP-*co*-AM-*co*-BAA) monolith was measured on a Zeiss ULTRA 55
169 field emission scanning electron microscope (Carl Zeiss AG, Oberkochen, Germany).
170 A mercury porosimetry Pore Master GT-60 (Quantachrome Instrument Corp., Boynton
171 Beach, FL, USA) was adopted to characterize the pore size distribution of the
172 poly(EGMP-*co*-AM-*co*-BAA) monolith. A ZEISS AXIO Observer A1 optical inverted
173 fluorescence microscope (Carl Zeiss AG, Oberkochen, Germany) equipped with a 20 \times
174 objective lens and coupled to an illuminator HXP 120C mercury lamp (Carl Zeiss AG,
175 Oberkochen, Germany) was used to detect the fluorescence on the poly(EGMP-*co*-AM-
176 *co*-BAA) monolith. The fluorescence detection was performed with a blue filter
177 (excitation 460-490 nm and emission 505-555 nm). A SP-403-M1 nanobaume capillary
178 column packer (Western Fluids Engineering and Manufacturing, Wildomar, CA, USA)
179 was employed for rinsing the capillary. The capillaries were connected to the capillary

180 column packer by means of a stainless-steel internal union fitted with a PEEK adapter.
181 Loading and elution times were optimized using the Zetalif LED induced fluorescence
182 (LED-LIF) detector (Picometrics Technologies, Toulouse, France) with the
183 PowerChrom 181 system (eDAQ Pty Ltd, Sydney, Australia). All CE experiments
184 (including the off-line analyses and on-line ones) were performed on the P/ACE MDQ
185 capillary electrophoresis device (SCIEX, Brea, CA, USA) equipped with a LIF detection
186 module ($\lambda_{\text{ex}} = 488 \text{ nm}$, $\lambda_{\text{em}} = 520 \text{ nm}$) but in two different laboratories. The CE-LIF data
187 were collected and processed with 32 Karat software (SCIEX).

188

189 **2.3 Preparation of Zr^{4+} modified poly(EGMP-*co*-AM-*co*-BAA) monolith**

190 Prior to polymerization, the UV transparent capillary was pretreated with γ -MAPS
191 according to previously published work [35]. In brief, new capillaries were rinsed with
192 1 M NaOH solution for 30 min, water for 10 min, 0.1 M HCl solution for 30 min, water
193 for 10 min and acetone for 15 min in turns. All the above risings were conducted at 3
194 bars using the capillary column packer system. Then, the treated capillaries were dried
195 in an oven (120 °C for 2 h) under nitrogen stream at 3 bars. After that, the capillaries
196 were refilled with 50% γ -MAPS solution in acetone (v/v). Both ends of the capillaries
197 were sealed with rubber septas and kept in the oven at 100 °C for 2 h. Afterwards, the
198 capillaries were kept in darkness overnight at room temperature. Finally, the capillaries
199 were rinsed with MeOH for 15 min and dried under nitrogen for 1 h at 3 bars.

200 The poly(EGMP-*co*-AM-*co*-BAA) monolithic column was synthesized following the
201 previously reported method [34]. In short, the polymerization mixture consisting of

202 EGMP (80 μL), AM: BAA mixture (60 mg), dodecanol (200 μL), DMSO (270 μL),
203 DMF (50 μL) and AIBN (2 mg) was mixed in a 2-mL vial. After sonication for 20 min
204 and bubbling with nitrogen for 10 min to remove dissolved gases, the mixture was
205 introduced into the pretreated capillary at a length of 10 cm. Both ends of the capillary
206 were sealed with rubber septas. The capillary was then irradiated by UV light at 365
207 nm with a light intensity of 1.5 mW cm^{-2} for 15 min. The distance between the capillary
208 and light source was 15 cm. To remove the porogen solvents and any other unreacted
209 reagents after polymerization, the monolithic column was rinsed with methanol and
210 water at 4 bars for 1 h and 15 min, respectively.

211 To immobilize Zr^{4+} ions on the monolith, the prepared poly(EGMP-*co*-AM-*co*-BAA)
212 monolith was first rinsed with 100 mM ZrOCl_2 aqueous solution for 1 h at room
213 temperature. Then, both ends of the capillary were sealed with rubber septas and kept
214 in darkness at 25 $^{\circ}\text{C}$ for 24 h. Finally, the Zr^{4+} modified monolith was cut into small
215 pieces (2 cm each) and rinsed with water for 20 min to remove any residual Zr^{4+} ions.
216 All the rinsing steps were conducted at 3 bars using the capillary column packer. The
217 Zr^{4+} modified poly(EGMP-*co*-AM-*co*-BAA) monolith was then ready to use.

218

219 **2.4. Sample preparation**

220 Preparation of the APTS labeled maltooligosaccharide ladder was as follows. 2.0 mg
221 of maltooligosaccharide ladder was weighed into a 200 μL eppendorf tube. Then 4 μL
222 of 40 mM APTS in 20% acetic acid, 4 μL of 20% acetic acid and 2 μL of 1M NaBH_3CN
223 in THF were added in the tube and the mixture was incubated for 30 min at 70 $^{\circ}\text{C}$ with

224 the tube open (evaporative labeling [36]). After incubation, the residues were dissolved
225 in 100 μL of water to obtain the solution of APTS labeled sugars (20 mg mL^{-1}) and the
226 labeled ladder solution was stored at $4 \text{ }^\circ\text{C}$. For off-line and on-line IMAC enrichment
227 and direct CE-LIF analysis, the maltooligosaccharide sample was first diluted with
228 water by 1000x and then with 0.0125% formic acid solution by 100x.

229 RNase B derived N-glycan preparation started with the addition of $5.0 \text{ } \mu\text{L}$ of
230 denaturation solution from the Fast Glycan Labeling and Analysis Kit to $10 \text{ } \mu\text{L}$ of 10
231 mg mL^{-1} aqueous RNase B solutions. The denaturation step proceeded for 10 min at
232 $70 \text{ }^\circ\text{C}$. Then, $12.0 \text{ } \mu\text{L}$ of water and $5.0 \text{ } \mu\text{L}$ of PNGase F (1.5 mU) was added to the
233 mixture. After mixing and incubation at $50 \text{ }^\circ\text{C}$ for 60 min, the sample was mixed with
234 the magnetic cleanup beads of the Fast Glycan Labeling and Analysis Kit and vortexed
235 for 10 s at the maximum speed. Then, $200 \text{ } \mu\text{L}$ of ACN was added into the sample tube
236 and mixed for 10 s with vortex. After 1 min, the supernatant was removed using a
237 magnetic stand. After that, the labeling solution containing $4.0 \text{ } \mu\text{L}$ of 40 mM APTS in
238 20% acetic acid, $2.0 \text{ } \mu\text{L}$ of NaBH_3CN (1 M in THF), $4.0 \text{ } \mu\text{L}$ of 20% acetic acid and 5.0
239 μL of THF was added in the sample tube and mixed for 1 min. The reaction mixtures
240 were incubated in a heating block at $50 \text{ }^\circ\text{C}$ in a closed vial (no evaporation) for 60 min
241 and another 60 min in an open lid vial (evaporative labeling) vials [36]. After the
242 labeling step, the samples were magnetic bead purified with $200 \text{ } \mu\text{L}$ of ACN-water
243 (90:10) solution three times, eluted by $50 \text{ } \mu\text{L}$ of water (2 mg mL^{-1}) and stored at $4 \text{ }^\circ\text{C}$.
244 For IMAC enrichment and CE-LIF analysis, the RNase B derived N-glycan sample was
245 diluted with 0.0125% formic acid solution by 1000x.

246

247 **2.5. Capillary Electrophoresis**

248 A fused silica capillary with an i.d. of 50 μm (o.d. 375 μm) and a total length of 30 cm
249 (effective length of 20 cm) was used to perform the separation. The cartridge and
250 sample plate were thermostated at 25 $^{\circ}\text{C}$. Before the first use, a new capillary was
251 pretreated by flushing with deionized water for 2 min, 1 M NaOH for 2 min, 1 M HCl
252 for 2 min and deionized water for 5 min, successively. A 25 mM lithium acetate buffer
253 (pH 4.75) was used as background electrolyte (BGE) for the separation. For off-line
254 preconcentration, the capillary was rinsed before each analysis with the BGE for 3 min.
255 All rinsing procedures were performed at 20 psi. Separation was achieved at a voltage
256 of 30 kV ($1000 \text{ V}\cdot\text{cm}^{-1}$, reversed polarity) with a current of approximately 38 μA . For
257 on-line preconcentration and CE-LIF analysis of APTS-maltooligosaccharides, the
258 separation was carried out at 15 kV ($500 \text{ V}\cdot\text{cm}^{-1}$, reversed polarity) with a current of
259 approximately 18.5 μA .

260

261 **2.6 Off-line and on-line preconcentration and CE-LIF analysis of APTS-glycans**

262 Off-line experiments consisting of the loading, rinsing, elution and separation of the
263 glycan mixture were performed under optimized conditions for each step. The loading
264 step was performed by flushing the monolith with APTS-glycans solubilized in the
265 loading buffer (0.0125% formic acid- H_2O) using the capillary column packer at 8 bars
266 for 32 min. The monolith was then rinsed with 0.0125% formic acid / 20% ACN in
267 H_2O solution using the capillary column packer at 8 bars for 5 min. The enriched

268 glycans were finally eluted with 0.03% ammonium hydroxide solution (pH 10.9) using
269 the capillary column packer at 8 bars for 2 min. Then the elution fraction was analyzed
270 by CE-LIF.

271 For on-line preconcentration and CE-LIF analysis of APTS-maltooligosaccharides,
272 a freshly made 3-mm capillary piece containing IMAC-Zr⁴⁺ monolith was first
273 connected to the inlet end of the separation capillary by a 10-mm-long PTFE tube (**Fig**
274 **S-1**). Then, the capillary system was flushed with 0.125% HCOOH-H₂O at 80 psi for 1
275 min as a leakage test to insure any bubble formation and avoid current breakdown
276 during the separation. For loading, APTS-labeled maltooligosaccharides were
277 dissolved in 0.125% HCOOH-H₂O and filled from the inlet end at 10 psi for 10 min
278 until the fluorescence reached a plateau. After that, the capillary was rinsed by 0.0125%
279 HCOOH / 20% ACN in H₂O at 20 psi until the fluorescence dropped to zero (around
280 8-10 min). Then, the system was filled with the BGE at 80 psi for 1 min from the inlet
281 end and the elution solution (0.3% NH₃-H₂O) was injected at 5 psi for 5 sec before
282 applying voltage for CE-LIF.

283 For off-line and on-line studies, CE-LIF analyses were performed in two different
284 laboratories. Electrophoregrams were displayed using relative and non-normalized
285 fluorescence Y-axis.

286

287 **3 RESULTS AND DISCUSSION**

288 Our group recently reported successful on-line IMAC-enrichment of
289 phosphopeptides in a glass microchip using a poly(EGMP-co-AM-co-BAA) monolith

290 bearing phosphate groups and functionalized with Zr^{4+} [34]. Therefore, we explored the
291 possibility to use a similar type of phosphate-containing monolith to enrich APTS-
292 labeled N-glycans by adapting its synthesis to a capillary format. Although according
293 to the « Hard and Soft Acids and Bases » concept [37] the interaction between hard
294 Lewis acid (Zr^{4+}) and soft Lewis base (sulfonate) is not expected to be stable as hard
295 acid (Zr^{4+}) - hard base (phosphate). To allow successful IMAC enrichment of APTS-
296 glycans, we therefore put some efforts in finding conditions strengthening the affinity
297 between Zr^{4+} and sulfonate groups brought by APTS. This is of the utmost importance
298 as APTS bearing several negative charges is the only tagging dye of glycans to allow
299 their analysis by CE. This IMAC enrichment was then on-line coupled to a CE-LIF
300 separation.

301

302 **3.1 Preparation and characterization of the poly(EGMP-co-AM-co-BAA)** 303 **monolith**

304 The reactive mixture previously reported for the monolith synthesis in microchips
305 was adapted to the fused silica capillary format. First the capillary walls were treated
306 with γ -MAPS using the protocol already reported [34]. A slight increase of the
307 monomers to porogen ratio was necessary so as to obtain a homogenous and well
308 anchored monolith. The obtained poly(EGMP-co-AM-co-BAA) monolith was
309 characterized by SEM. A tight anchoring of the monolithic bed onto the inner wall of
310 the γ -MAPs pretreated capillary was observed. Large through-pores and a continuous
311 skeleton were also observed.

312 Mercury intrusion porosimetry (MIP) results exhibited a broad monomodal
313 distribution with most pores in the size range from 0.34 to 2.34 μm and a maximum at
314 0.76 μm , corresponding to a total pore volume of 0.159 $\text{cm}^3 \text{g}^{-1}$. Such macro-pores could
315 provide sufficiently high permeability and concomitantly low backpressure. The
316 specific surface area was 8.8 $\text{m}^2 \text{g}^{-1}$.

317 When plotting backpressure versus flow rate for a 2-cm monolith column, good
318 linear relationships ($R^2 > 0.991$) were obtained in the pressure range from 13 to 117
319 bars, depending on the nature of the mobile phase used. In addition, neither crack nor
320 detachment of the monolith from the capillary wall was observed under high pressures.
321 These observations suggest a homogeneous pore structure along the monolithic column
322 and an excellent mechanical stability. **Table 1** shows the permeability values of the
323 poly(EGMP-*co*-AM-*co*-BAA) monolith evaluated according to Darcy's law (SI 2) by
324 using MeOH, MeOH/H₂O (50/50, v/v), ACN or H₂O as the mobile phase. It is worth
325 noting that these values were similar, indicating the good wettability and chemical
326 stability (neither swelling nor shrinking of the monolith) in the various solvents used
327 with quite different polarities.

328

329 **3.2 IMAC enrichment of the APTS labeled maltooligosaccharide ladder**

330 The IMAC-sorbent based on the poly(EGMP-*co*-AM-*co*-BAA) monolith was
331 prepared by simply immobilizing Zr^{4+} on its phosphate surface via metal chelation [34].
332 In accordance with the metal (IV) and the sulfonate chemistry, the three oxygens of
333 each sulfonate group of the APTS (linked to glycans) could be octahedrally coordinated

334 by three Zr^{4+} . Therefore, the Zr^{4+} modified poly(EGMP-*co*-AM-*co*-BAA) monolith
335 could be used to enrich specifically APTS labeled glycans via strong interactions.

336 The affinity of the Zr^{4+} modified poly(EGMP-*co*-AM-*co*-BAA) monolith for APTS
337 was first demonstrated by loading an APTS solution on both Zr^{4+} modified and
338 unmodified monoliths. After the rinsing step, high fluorescence was observed on the
339 Zr^{4+} modified poly(EGMP-*co*-AM-*co*-BAA) monolith, while no fluorescence was
340 visible on the unmodified one. This indicates that the prepared Zr^{4+} modified
341 poly(EGMP-*co*-AM-*co*-BAA) monolith has a good selectivity toward APTS.

342 The performance of the Zr^{4+} modified poly(EGMP-*co*-AM-*co*-BAA) monolith for
343 preconcentration of APTS-glycans was then evaluated using the APTS labeled
344 maltooligosaccharide ladder. The pH of the loading and elution solutions significantly
345 affected the efficiency of the enrichment. To avoid precipitation of $ZrOCl_2$ at alkaline
346 conditions, the pH of the loading solution was kept under 4.0 [38]. This is compatible
347 with an efficient capture of glycans as their interaction with Zr^{4+} is influenced by the
348 charge of APTS that is negative whatever the pH (negative pKa). Moreover, to allow
349 sufficient separation of the APTS-maltooligosaccharide ladder during the off-line CE
350 analysis, very low acid content in the loading buffer was required. Various formic acid
351 aqueous solutions (ranging from 0.0125% to 3%) with a pH lower than 3.3 were tested.
352 In the case of APTS-maltooligosaccharide samples, 0.0125% formic acid- H_2O (pH 3.3)
353 was found acidic enough to make sure the Zr^{4+} modified monolith can efficiently
354 capture the APTS-sugars and was therefore selected as loading solution.

355 The capture of maltooligosaccharides was monitored in the middle of the monolith

356 using an epifluorescence microscope (Fig S-2A). Before loading the sample, no
357 fluorescence was detected (**Fig. 1A**). After sample loading and rinsing with 20% ACN-
358 H₂O containing 0.0125% formic acid, fluorescence was detected on the monolith (**Fig.**
359 **1B**). These results demonstrated the efficient capture of the APTS-
360 maltooligosaccharides via strong interactions between the sulfonate groups of the APTS
361 and the Zr⁴⁺ modified monolith. This is particularly interesting since affinity between
362 soft Lewis base and hard Lewis acid tends to be generally weak. As previous studies
363 showed that elution solutions containing strong chelating agents like ammonium
364 favored the elution of the captured phosphopeptides after an IMAC-enrichment [34],
365 different ammonium hydroxide solutions (from 0.0003% to 0.3%) were tested to elute
366 the APTS-labeled sugars. Indeed, the interaction APTS-Zr⁴⁺ (soft Lewis base - hard
367 Lewis acid) is weaker than the ammonium-Zr⁴⁺ (hard Lewis base - hard Lewis acid).
368 Elution efficiency was assessed (Fig S-3). Most of the captured APTS-
369 maltooligosaccharides were eluted when the Zr⁴⁺ modified poly(EGMP-*co*-AM-*co*-
370 BAA) monolith was rinsed with 0.03% (pH 10.9) or 0.3% ammonium hydroxide (pH
371 11.5). However, to avoid any potential damage of the monolith and to have a pH
372 condition compatible with the subsequent CE separation, 0.03% ammonium hydroxide
373 was selected as elution solution, ensuring dramatic decrease in the fluorescence
374 intensity as shown in **Fig. 1C**. The elution efficiency was estimated to be 82.7% (SI 3).
375 The reproducibility of the entire enrichment procedure, starting from Zr⁴⁺
376 immobilization to APTS-maltooligosaccharide elution, was investigated on three
377 different monoliths and the RSD of elution efficiency was found to be very good (<

378 3.0%). The developed IMAC-method based on the Zr^{4+} modified poly(EGMP-*co*-AM-
379 *co*-BAA) monolith can therefore enrich the APTS labeled maltooligosaccharide ladder
380 with high efficiency and reproducibility.

381 The reusability of the Zr^{4+} modified poly(EGMP-*co*-AM-*co*-BAA) monolith was
382 also evaluated. Two consecutive enrichment processes (capture, rinsing and elution)
383 were performed on the same monolith where the Zr^{4+} was immobilized only once. After
384 the sample loading and rinsing procedure, the fluorescence intensity on the monolith
385 was dramatically reduced (by a factor of four) between the first and the second run,
386 suggesting a significant loss in loading efficiency. This could be attributed to the
387 repetitive washings with acidic and alkaline solutions that might partly remove the Zr^{4+}
388 ions from the monolith. Wang *et al* who also used a Zr^{4+} modified monolith but for
389 phosphopeptide enrichment stated that dissociation of Zr^{4+} -phosphate bonds could be
390 provoked by the continuous introduction during washings and elutions of Lewis bases,
391 which are stronger than phosphate groups [35]. Although this can be a disadvantage of
392 the non-permanent binding method, the optimized enrichment method allowed reaching
393 high efficiency and reproducibility when performing the whole IMAC process starting
394 from the Zr^{4+} immobilization step with no need to prepare again a new monolith as it is
395 stable enough. Moreover, the immobilization step could be significantly shortened
396 when dealing with shorter length plugs of monolith.

397 The loading and elution times were also optimized as they are expected to
398 significantly influence the enrichment efficiency. The Zr^{4+} modified poly(EGMP-*co*-
399 AM-*co*-BAA) monolith was connected on-line via an empty capillary to a LIF detector

400 located at 10 cm after the monolith (Fig S-2B). The fluorescence intensity was recorded
401 over 55 min and plotted as a function of time during the loading step (SI 4). The optimal
402 loading time, defined as the time necessary to saturate the Zr^{4+} modified monolith with
403 the APTS-maltooligosaccharide ladder and reach the plateau of fluorescence intensity,
404 was approximately 32 min (**Fig. 2A**). The reproducibility of this loading time was
405 evaluated on three batches of the Zr^{4+} modified poly(EGMP-*co*-AM-*co*-BAA)
406 monoliths (RSD = 6.9%). After rinsing with 0.0125% formic acid-20% ACN-H₂O for
407 5 min at 8 bars, the elution step was also recorded (SI 4). The signal dropped to the
408 baseline level after 2 min of elution, indicating an efficient desorption of the APTS-
409 maltooligosaccharide ladder (**Fig. 2B**). Therefore, the optimal time for elution was set
410 at 2 min (6.8% RSD, n = 3).

411 The performances of the IMAC-preconcentration in terms of selectivity and signal
412 enrichment factor were evaluated. Solutions of the APTS-maltooligosaccharide ladder
413 collected during different steps of the entire enrichment procedure were analyzed by
414 CE-LIF. The profile obtained after off-line preconcentration (**Fig. 3d**) showed much
415 higher peak intensities than the profile of the loading solution (**Fig. 3a**), demonstrating
416 that the Zr^{4+} -monolith can enrich all APTS-oligomers regardless of their size. Moreover,
417 the very low peak intensity obtained for the solutions recovered during the loading (**Fig.**
418 **3b**) and rinsing (**Fig. 3c**) steps clearly indicated efficient capture and rinsing. As shown
419 in **Fig. 4**, the signal enrichment factors evaluated by comparing the peak area with and
420 without preconcentration (SI 2) and ranging from 9.3 to 24.2 were not the same for the
421 different glucose oligomers. The lowest one (9.3) was obtained for the glucose

422 monomer (G1) whereas it was twice or 2.5-fold higher for the other oligomers. Big size
423 oligomers may be more flexible and this could favor their affinity for the Zr⁴⁺-monolith.
424 The drop at G8 was probably due to the conformation change from random coil to well
425 defined helical structure as was suggested earlier [39]. Nevertheless, this similar
426 selectivity of the monolith for oligomers presenting a size higher than 2 glucose units
427 (GU) and lower than 15 is therefore well suited for the glycoprotein-derived N-glycans
428 since the size of most plasma glycoprotein N-linked sugars usually ranges from 4 to 15
429 GU [40]. The reproducibility of enrichment factors was evaluated by repeating the
430 experiments on three different Zr⁴⁺-monoliths, which were cut from the same monolith
431 and modified with Zr⁴⁺ separately. We observed very low RSD for peak area for glucose
432 (2.0%), this value increased to 4.0-9.2% for G2 to G11 and decreased again for longer
433 glucose oligomers above G12 (RSD from 3.1 to 4.7%). Finally, very good
434 repeatabilities (less than 6.7%) were obtained for glucose oligomers corresponding to
435 sizes expected for N-glycans, demonstrating interesting potentials of this Zr⁴⁺ modified
436 monolith for further purification or enrichment of APTS labeled N-glycans from
437 glycoproteins.

438

439 **3.3. IMAC enrichment of APTS labeled RNase B N-glycans**

440 To further evaluate the performance of the Zr⁴⁺ modified poly(EGMP-*co*-AM-*co*-
441 BAA) monolith for glycan enrichment, the optimized preconcentration procedure was
442 applied to enrich N-glycans released from ribonuclease B (RNase B) by PNGase F
443 digestion and labeled with APTS. The initial sample was percolated (32 min under 8

444 bars) through the Zr^{4+} modified poly(EGMP-*co*-AM-*co*-BAA) monolith. As expected
445 and due to the very low concentration (under the detection limit of the CE-LIF), no
446 glycan was detected (**Fig. 5a**). For the same reason, a similar profile was observed for
447 the solution collected after the loading (**Fig. 5b**). The Zr^{4+} modified monolith was then
448 washed with 20% ACN in 0.0125% formic acid- H_2O and **Fig. 5c** shows the CE profile
449 obtained for the solution resulting from this rinsing. A few small APTS-glycan
450 conjugates were detected, demonstrating that they were not specifically retained on the
451 monolith. Finally, the retained glycans were eluted using 0.03% ammonium hydroxide,
452 collected and also analyzed by CE. As shown in **Fig. 5d**, all five expected oligomannose
453 glycans (Man 5 to Man 9) were successfully enriched at a detectable level with good
454 resolution as the three positional isomers of Man 7 (Peaks 3, 3* and 3**) and Man 8
455 (Peaks 4, 4* and 4**) were well separated. The profile was similar to the expected peak
456 distribution published earlier [41]. The relative peak area of each of the five N-glycans
457 after the enrichment were compared to those reported in the literature (**Table 2**) [42-
458 **44**]. The observed values are quite close to the literature values, confirming that the
459 monolith-based enrichment exhibits the same selectivity toward the different glycans.

460

461 **3.4. On-line preconcentration and CE-LIF analysis of APTS labeled** 462 **maltooligosaccharides**

463 This novel enrichment method of glycans, involving the use of monolith easy to
464 synthesize in capillaries and APTS, the fluorescent dye mostly employed in CE-LIF of
465 glycans, offered high potential for on-line coupling of enrichment and separation of

466 glycans. Along the above described off-line preconcentration method, the on-line
467 approach has then been exploited at the proof of concept level. A 3-mm capillary
468 containing monolith was directly connected to the inlet end of the separation capillary
469 by a PTFE tubing. The enrichment was achieved using the off-line conditions and the
470 fluorescence intensity was recorded during the loading step. The plateau was reached
471 in 2-3 minutes, much faster than during the off-line process, probably because of the
472 shorter monolith length. Then, the capillary was filled with the separation and elution
473 buffers and the sample was eluted directly into the separation capillary. Additional
474 preliminary experiments using an epifluorescence microscope showed that the
475 separation buffer did not elute the analytes from the monolith. The separation was then
476 carried out as with a conventional sample injection. A slight delay in the migration time
477 was observed for the on-line enrichment profile probably due to the additional 3-mm
478 capillary containing monolith (**Fig. 6**). Higher peak intensities were experienced with
479 on-line preconcentration compared to conventional sample injection. The average
480 enrichment factor was 5.5 for G1 to G15, with the highest value of 9.0 for G2 and the
481 lowest of 3.2 for G7. Except for G1 (which exhibited the lowest signal enrichment
482 factor in off-line enrichment), the values were approximately 4-fold lower for all
483 oligomers in comparison to the off-line method. The differences in enrichment factors
484 could be caused by the peak deformations observed for glucose oligomers bigger than
485 G5 that made the accurate peak area estimation difficult. Due to the complexity of the
486 on-line setup, repeatability experiments often resulted in relative high variance thus the
487 reported technique calls for to further optimization. For example, some commercial

488 fluid routing connectors and fittings, providing leak-free connectivity, even at high
489 pressures and exhibiting low dead volumes could be used to improve the connection
490 between the monolith column and the separation capillary. These very promising results
491 demonstrate however the first proof of concept of the possibility to couple on-line
492 labeled N-glycan enrichment and CE-LIF separation.

493

494 **4. Conclusion**

495 In this study, we introduced a new sample enrichment tool for APTS-labeled N-
496 glycans. The IMAC-preconcentration process was based on the use of an unexpected
497 but strong interaction between Zr^{4+} immobilized on the poly(EGMP-co-AM-co-BAA)
498 monolith with the sulfonate group brought by APTS. The loading (0.0125% formic
499 acid - H₂O, pH 3.3) and elution (0.03% ammonium hydroxide, pH 10.9) buffers were
500 able to respectively capture and elute the APTS-labeled maltooligosaccharides, leading
501 to a high enrichment efficiency (83%) without being detrimental to their CE separation
502 and regardless of the oligomer size. This latter feature is particularly interesting to
503 provide accurate estimation when seeking changes in the relative abundance of glycans
504 from a given glycoprotein. The relatively good enrichment factors (up to 24) for glucose
505 oligomers with good repeatabilities (<6.7%) suggest high performance of the
506 introduced preconcentration method. The five main N-glycans from the ribonuclease B
507 PNGase F digest were successfully enriched and detected by CE-LIF, without any bias
508 regarding their relative abundance. Here, the reported on-line coupling of the IMAC
509 monolith-based N-glycan enrichment with CE-LIF separation is the first demonstration

510 of this novel approach. The utilization of the IMAC method ensures better selectivity
511 in APTS-labeled glycan enrichment in comparison to commercial SPE columns
512 composed of HILIC or PGC materials. Thanks to the on-line process the IMAC based
513 on-line enrichment avoids losing any possible sample due to the coupling thus subjected
514 to broad interest when dealing with limited sample availability. Furthermore, as each
515 preconcentration step applies a new piece of the monolith, only a few mm long (ca. 15
516 cm long EGMP-co-AM-co-BAA monolith) can be prepared at the same time. Thus, the
517 developed method overcomes the carry-over problem of conventional preconcentration
518 techniques [45]. It is also readily applicable in most academic and industrial labs since
519 the monolith can be cut into small pieces for multiple preconcentration experiments.

520

521 **5. Acknowledgements**

522 This work was supported by China Scholarship Council (Grant No. 201700260121
523 and 201700260135) and by the international PHC Balaton (40480RH) and Cai Yuan
524 Pei (38914PC) programs. Part of this work was supported by a public grant overseen
525 by the French National Research Agency (ANR) as part of the “Investissements
526 d’Avenir” program (Labex NanoSaclay, reference: ANR-10-LABX-0035) and also the
527 departments of “Sciences de la Vie” and of “Chimie” of Université Paris-Saclay. This
528 is contribution #165 from the Horváth Csaba Memorial Laboratory of Bioseparation
529 Sciences. This work was also sponsored by the BIONANO_GINOP-2.3.2-15-2016-
530 00017 project and by the János Bolyai Research Scholarship as well as the ÚNKP-19-
531 4 New National Excellence Program of Hungarian Ministry for Innovation and

532 Technology. We thank the English teacher of the Faculty of Pharmacy B. Trimbach for
533 English proofreading.

534

535 **6. References**

536 [1] K. Ohtsubo, J.D. Marth, Glycosylation in cellular mechanisms of health and disease,
537 Cell 126 (2006) 855-867.

538 [2] A. Helenius, M. Aebi, Intracellular functions of N-linked glycans, Science 291
539 (2001) 2364-2369.

540 [3] J.W. Dennis, I.R. Nabi, M. Demetriou, Metabolism, cell surface organization, and
541 disease, Cell 139 (2009) 1229-1241.

542 [4] H.H. Freeze, J.X. Chong, M.J. Bamshad, B.G. Ng, Solving glycosylation disorders:
543 fundamental approaches reveal complicated pathways, Am. J. Hum. Genet. 94
544 (2014) 161-175.

545 [5] Y. Kizuka, S. Kitazume, N. Taniguchi, N-glycan and Alzheimer's disease, Biochim.
546 Biophys. Acta Gen. Subj. 1861 (2017) 2447-2454.

547 [6] B. Adamczyk, T. Tharmalingam, P.M. Rudd, Glycans as cancer biomarkers,
548 Biochim. Biophys. Acta 1820 (2012) 1347-1353.

549 [7] R. Testa, V. Vanhooren, A.R. Bonfigli, M. Boemi, F. Olivieri, A. Ceriello, S.
550 Genovese, L. Spazzafumo, V. Borelli, M.G. Bacalini, S. Salvioli, P. Garagnani, S.
551 Dewaele, C. Libert, C. Franceschi, N-Glycomic changes in serum proteins in type
552 2 diabetes mellitus correlate with complications and with metabolic syndrome
553 parameters, PLoS One 10 (2015) e0119983.

- 554 [8] X.E. Liu, L. Desmyter, C.F. Gao, W. Laroy, S. Dewaele, V. Vanhooren, L. Wang, H.
555 Zhuang, N. Callewaert, C. Libert, R. Contreras, C.Y. Chen, N-glycomic changes
556 in hepatocellular carcinoma patients with liver cirrhosis induced by hepatitis B
557 virus, *Hepatology* 46 (2007) 1426-1435.
- 558 [9] A.V. Everest-Dass, M.T. Briggs, G. Kaur, M.K. Oehler, P. Hoffmann, N.H. Packer,
559 N-glycan MALDI imaging mass spectrometry on formalin-fixed paraffin-
560 embedded tissue enables the delineation of ovarian cancer tissues, *Mol. Cell.*
561 *Proteomics* 15 (2016) 3003-3016.
- 562 [10] G.Y. Qing, J.Y. Yan, X.N. He, X.L. Li, X.M. Liang, Recent advances in hydrophilic
563 interaction liquid interaction chromatography materials for glycopeptide
564 enrichment and glycan separation, *Trac-Trend Anal. Chem.* 124 (2020) 115570.
- 565 [11] V. Mantovani, F. Galeotti, F. Maccari, N. Volpi, Recent advances in capillary
566 electrophoresis separation of monosaccharides, oligosaccharides, and
567 polysaccharides, *Electrophoresis* 39 (2018) 179-189.
- 568 [12] M.J. Kailemia, G.G. Xu, M. Wong, Q.Y. Li, E. Goonatileke, F. Leon, C.B. Lebrilla,
569 Recent advances in the mass spectrometry methods for glycomics and cancer, *Anal.*
570 *Chem.* 90 (2018) 208-224.
- 571 [13] J. Wei, Y. Tang, Y. Bai, J. Zaia, C.E. Costello, P.Y. Hong, C. Lin, Toward automatic
572 and comprehensive glycan characterization by online PGC-LC-EED MS/MS,
573 *Anal. Chem.* 92 (2020) 782-791.
- 574 [14] Y.Y. Qu, L.L. Sun, Z.B. Zhang, N.J. Dovichi, Site-specific glycan heterogeneity
575 characterization by hydrophilic interaction liquid chromatography solid-phase

576 extraction, reversed-phase liquid chromatography fractionation, and capillary
577 zone electrophoresis-electrospray ionization-tandem mass spectrometry, *Anal.*
578 *Chem.* 90 (2018) 1223-1233.

579 [15] S. Yamamoto, M. Kinoshita, S. Suzuki, Current landscape of protein glycosylation
580 analysis and recent progress toward a novel paradigm of glycoscience research, *J.*
581 *Pharm. Biomed. Anal.* 130 (2016) 273-300.

582 [16] Y. Zhang, X.F. Wu, W. A. Tao, Characterization and applications of extracellular
583 vesicle proteome with post-translational modifications, *Trends Analyt. Chem.* 107
584 (2018) 21-30.

585 [17] N.R. Sun, C.H. Deng, Y. Li, X.M. Zhang, Highly selective enrichment of N-linked
586 glycan by carbon-functionalized ordered graphene/mesoporous silica composites,
587 *Anal. Chem.* 86 (2014) 2246-2250.

588 [18] N.R. Sun, J.Z. Yao, C.H. Deng, Designed synthesis of carbon-functional magnetic
589 graphene mesoporous silica materials using polydopamine as carbon precursor for
590 the selective enrichment of N-linked glycan, *Talanta* 148 (2014) 439-443.

591 [19] J.N. Zheng, Y. Xiao, L. Wang, Z. Lin, H.H. Yang, L. Zhang, G.N. Chen, Click
592 synthesis of glucose-functionalized hydrophilic magnetic mesoporous
593 nanoparticles for highly selective enrichment of glycopeptides and glycans, *J.*
594 *Chromatogr. A* 1358 (2014) 29-38.

595 [20] S. Yamamoto, S. Suzuki, S. Suzuki, Microchip electrophoresis of oligosaccharides
596 using lectin-immobilized preconcentrator gels fabricated by in situ
597 photopolymerization, *Analyst* 137 (2012) 2211-2217.

- 598 [21] R.R. Xing, S.S. Wang, Z.J. Bie, H. He, Z. Liu, Preparation of molecularly
599 imprinted polymers specific to glycoproteins, glycans and monosaccharides via
600 boronate affinity controllable-oriented surface imprinting, *Nat. Protoc.* 12 (2017)
601 964-987.
- 602 [22] K. Fabijanczuk, K. Gaspar, N. Desai, J. Lee, D.A. Thomas, J.L. Beauchamp, J.S
603 Gao, Resin and magnetic nanoparticle-based free radical probes for glycan capture,
604 isolation, and structural characterization, *Anal. Chem.* 91 (2019) 15387-15396.
- 605 [23] D. Schemeth, M. Rainer, C.B. Messner, B.M. Rode, G.K. Bonn, Lanthanide-IMAC
606 enrichment of carbohydrates and polyols, *Biomed. Chromatogr.* 28 (2014) 412-
607 418.
- 608 [24] Y. Zhang, Y. Peng, Z.C. Bin, H.J. Wang, H.J. Lu, Highly specific purification of
609 N-glycans using phosphate-based derivatization as an affinity tag in combination
610 with Ti^{4+} -SPE enrichment for mass spectrometric analysis, *Anal. Chim. Acta* 934
611 (2016) 145-151.
- 612 [25] H.H. Bai, Y.T. Pan, W. Tong, W.J. Zhang, X.J. Ren, F. Tian, B. Peng, X. Wang, Y.J.
613 Zhang, Y.L. Deng, W.J. Qin, X.H. Qian, Graphene based soft nanoreactors for
614 facile “one-step” glycan enrichment and derivatization for MALDI-TOF-MS
615 analysis, *Talanta* 117 (2013) 1-7.
- 616 [26] J.C. Masini, F. Svec, Porous monoliths for on-line sample preparation: A review,
617 *Anal. Chim. Acta* 964 (2017) 24-44.
- 618 [27] M. Chen, Y. Lu, Q. Ma, L. Guo, Y.Q. Feng, Boronate affinity monolith for highly
619 selective enrichment of glycopeptides and glycoproteins, *Analyst* 134 (2009)

- 620 2158-2164.
- 621 [28] W.J. Zhang, N.Z. Song, H.J. Zheng, W. Feng, Q. Jia, Cobalt phthalocyanine
622 tetracarboxylic acid functionalized polymer monolith for selective enrichment of
623 glycopeptides and glycans, *Proteomics* 18 (2018) 1700399.
- 624 [29] M. Zhao, C.H. Deng, Fluorous modified magnetic mesoporous silica composites
625 incorporated fluorous solid-phase extraction for the specific enrichment of N-
626 linked glycans with simultaneous exclusion of proteins, *Talanta* 159 (2016) 111-
627 116.
- 628 [30] L.L. Li, J. Jiao, Y. Cai, Y. Zhang, H.J. Lu, Fluorinated carbon tag derivatization
629 combined with fluorous solid-phase extraction: a new method for the highly
630 sensitive and selective mass spectrometric analysis of glycans, *Anal. Chem.* 87
631 (2015) 5125-5131.
- 632 [31] M.H.J. Selman, M. Hemayatkar, A.M. Deelder, M. Wührer, Cotton HILIC SPE
633 microtips for microscale purification and enrichment of glycans and glycopeptides,
634 *Anal. Chem.* 83 (2011) 2492-2499.
- 635 [32] A. Koller, J. Khandurina, J. Li, J. Kreps, D. Schieltz, A. Guttman, Analysis of high-
636 mannose-type oligosaccharides by microliquid chromatography-mass
637 spectrometry and capillary electrophoresis, *Electrophoresis* 25 (2004) 2003-2009.
- 638 [33] P. Smejkal, A. Szekrenyes, M. Ryvolova, F. Foret, A. Guttman, F. Bek, M. Macka,
639 Chip-based CE for rapid separation of 8-aminopyrene-1,3,6-trisulfonic acid
640 (APTS) derivatized glycans, *Electrophoresis* 31 (2010) 3783-3786.
- 641 [34] M. Araya-Farias, S. Dziomba, B. Carbonnier, M. Guerrouache, I. Ayed, N. Aboud,

642 M. Taverna, N. Thuy Tran, A lab-on-a-chip for monolith-based preconcentration
643 and electrophoresis separation of phosphopeptides, *Analyst* 142 (2017) 485-494.

644 [35] H. Wang, J.C. Duan, H.J. Xu, L. Zhao, Y. Liang, Y.C. Shan, L.H. Zhang, Z. Liang,
645 Y.K. Zhang, Monoliths with immobilized zirconium ions for selective enrichment
646 of phosphopeptides, *J. Sep. Sci.* 34 (2011) 2113-2121.

647 [36] B. Reider, M. Szigetia, A. Guttman, Evaporative fluorophore labeling of
648 carbohydrates via reductive amination, *Talanta* 185 (2018) 365-369.

649 [37] R.G. Pearson, Hard and soft acids and bases, HSAB, part 1: Fundamental
650 principles, *J. Chem. Educ.* 45 (1968) 581-587.

651 [38] T. Kobayashi, T. Sasaki, I. Takagi, H. Moriyama, Solubility of zirconium (IV)
652 hydrous oxides, *J. Nucl. Sci. Technol.* 44 (2007) 90-94.

653 [39] M. Kerékgyártó, G. Járvas, L. Novák, A. Guttman, Activation energy associated
654 with the electromigration of oligosaccharides through viscosity modifier and
655 polymeric additive containing background electrolytes, *Electrophoresis* 37 (2016)
656 573-578.

657 [40] GU database, <https://lendulet.uni-pannon.hu/index.php/gudatabase>, 2019,
658 (accessed 26 November 2019).

659 [41] A. Guttman, T. Pritchett, Capillary gel electrophoresis separation of high-mannose
660 type oligosaccharides derivatized by 1-aminopyrene-3,6,8-trisulfonic acid,
661 *Electrophoresis* 16 (1995) 1906-1911.

662 [42] C. Varadi, C. Lew, A. Guttman, Rapid magnetic bead based sample preparation for
663 automated and high throughput N-glycan analysis of therapeutic antibodies, *Anal.*

664 Chem. 86 (2014) 5682-5687.

665 [43] M. Szigeti, J. Bondar, D. Gjerdec, Z. Keresztessy, A. Szekrenyes, A. Guttman,
666 Rapid N-glycan release from glycoproteins using immobilized PNGase F
667 microcolumns, J. Chromatogr. B 1032 (2016) 139-143.

668 [44] G. Chen, Q. Bai, X.D. Geng, Preparation of a concanavalin A immobilized affinity
669 column and its application in the structural analysis of ribonuclease B, Chin. J.
670 Chromatogr. 24 (2006) 425-431.

671 [45] D.M. Osbourn, D.J. Weiss, C.E. Lunte, On-line preconcentration methods for
672 capillary electrophoresis, Electrophoresis 21 (2000) 2768-2779.

673

Figure Caption

674

675 **Fig. 1** Fluorescent images of the Zr^{4+} modified poly(EGMP-*co*-AM-*co*-BAA)-monolith:
676 (A) capillary with monolith before the loading APTS-maltooligosaccharide sample, (B)
677 after loading the APTS-maltooligosaccharide at $0.2 \mu\text{g mL}^{-1}$ for 32 min and rinsing for
678 5 min and (C) after elution for 2 min. All loading, rinsing and elution procedures were
679 performed with the capillary column packer at 8 bars. Fluorescence detection: $\lambda_{\text{exc}} =$
680 495 nm, $\lambda_{\text{em}} = 525$ nm. Loading buffer: 0.0125% formic acid- H_2O (pH 3.3). Rinsing
681 buffer: 0.0125% formic acid-20% ACN- H_2O . Elution buffer: 0.03% ammonium
682 hydroxide (pH 10.9).

683 **Fig. 2** Typical fluorescence intensity profiles recorded during the loading (A) and
684 elution (B) steps of an APTS maltooligosaccharide ladder captured by the Zr monolith.
685 Fluorescence detection: $\lambda_{\text{exc}} = 480$ nm, $\lambda_{\text{em}} = 520$ nm. Concentration of APTS-
686 maltooligosaccharide ladder in loading solution (0.0125% formic acid- H_2O) was 0.2
687 $\mu\text{g mL}^{-1}$. Both loading and elution procedures were performed with the capillary
688 column packer at 8 bars.

689 **Fig. 3** CE-LIF separation of the APTS-maltooligosaccharide ladder starting solution
690 ($0.2 \mu\text{g mL}^{-1}$) before loading (a), in the solutions resulting from the loading (b), rinsing
691 (c) and elution (d) steps. Peaks: 0, APTS excess; 1-15, APTS labeled glucose oligomers
692 from 1 to 15 glucose units. Separation conditions: 25 mM lithium acetate buffer (pH
693 4.75); separation voltage: -30 kV; capillary: $50 \mu\text{m}$ i.d., 30 cm total length, 20 cm
694 effective length; temperature: 25°C ; LIF detection: $\lambda_{\text{exc}} = 488$ nm, $\lambda_{\text{em}} = 520$ nm.
695 Sample injection: 0.5 psi, 3s.

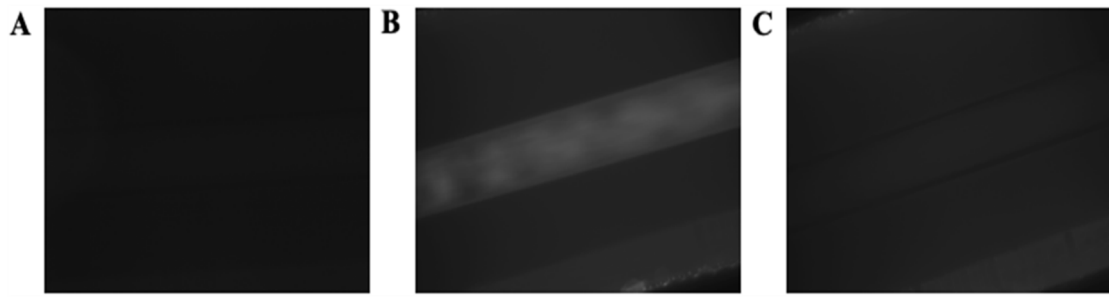
696 **Fig. 4** Signal enrichment factors of APTS-glucose oligomers on the Zr^{4+} modified
697 poly(EGMP-*co*-AM-*co*-BAA) monolith. In G_x: x represents the number of glucose
698 units. Error bars indicate SD from n=3 experiments.

699 **Fig. 5** CE-LIF of APTS labeled RNase B N-glycans ($2 \mu\text{g mL}^{-1}$). (a) Initial solution
700 before enrichment and solutions resulting from the (b) loading; (c) washing; (d) elution
701 fractions. Peaks 1 to 5 correspond to Man 5 to Man 9, peaks 3*, 3** and 4*, 4** are
702 the positional isomers of Man 7 and Man 8, respectively. CE-LIF conditions as in **Fig.**
703 **3**.

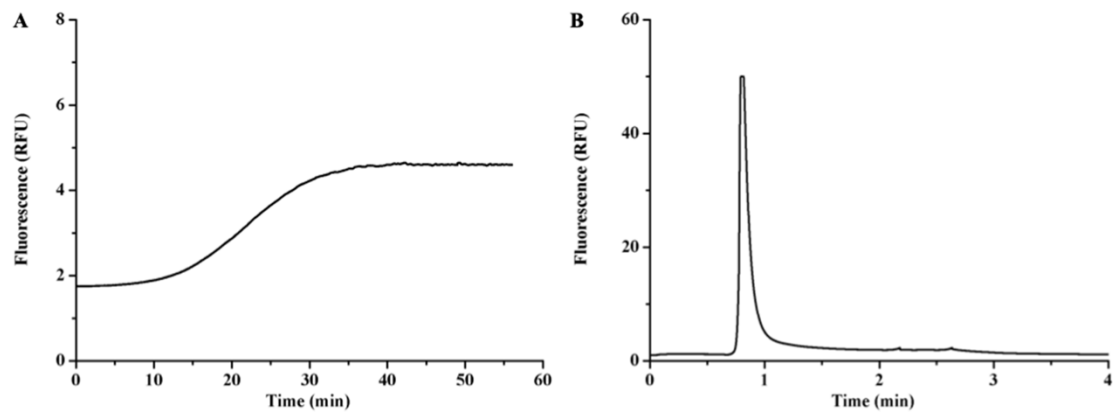
704 **Fig. 6** CE-LIF separation of APTS-maltooligosaccharide ladder ($0.2 \mu\text{g mL}^{-1}$) (a)
705 without preconcentration and (b) with on-line enrichment. Peaks: 0, APTS excess; 1-
706 20, APTS labeled glucose oligomers from 1 to 20 glucose units. Separation conditions:
707 25 mM LiAc (pH 4.75); separation voltage: -15 kV; capillary: 50 μm i.d., total/effective
708 length of 30/20 cm for (a) and 30.3/20.3cm for (b); temperature: 25°C; LIF detection:
709 $\lambda_{\text{exc}} = 488 \text{ nm}$, $\lambda_{\text{em}} = 520 \text{ nm}$. Sample enrichment procedures: (i) loading condition:
710 APTS-maltooligosaccharide ladder in 0.125% HCOOH-H₂O at 10 psi for 10 min; (ii)
711 rinsing with 0.0125% HCOOH / 20% ACN in H₂O) at 20 psi for 8 min; (iii) elution
712 with 0.3% NH₃-H₂O at 5 psi for 5 s.

713
714

715 **Fig. 1**



734 **Fig. 2**



735

736

737

738

739

740

741

742

743

744

745

746

747

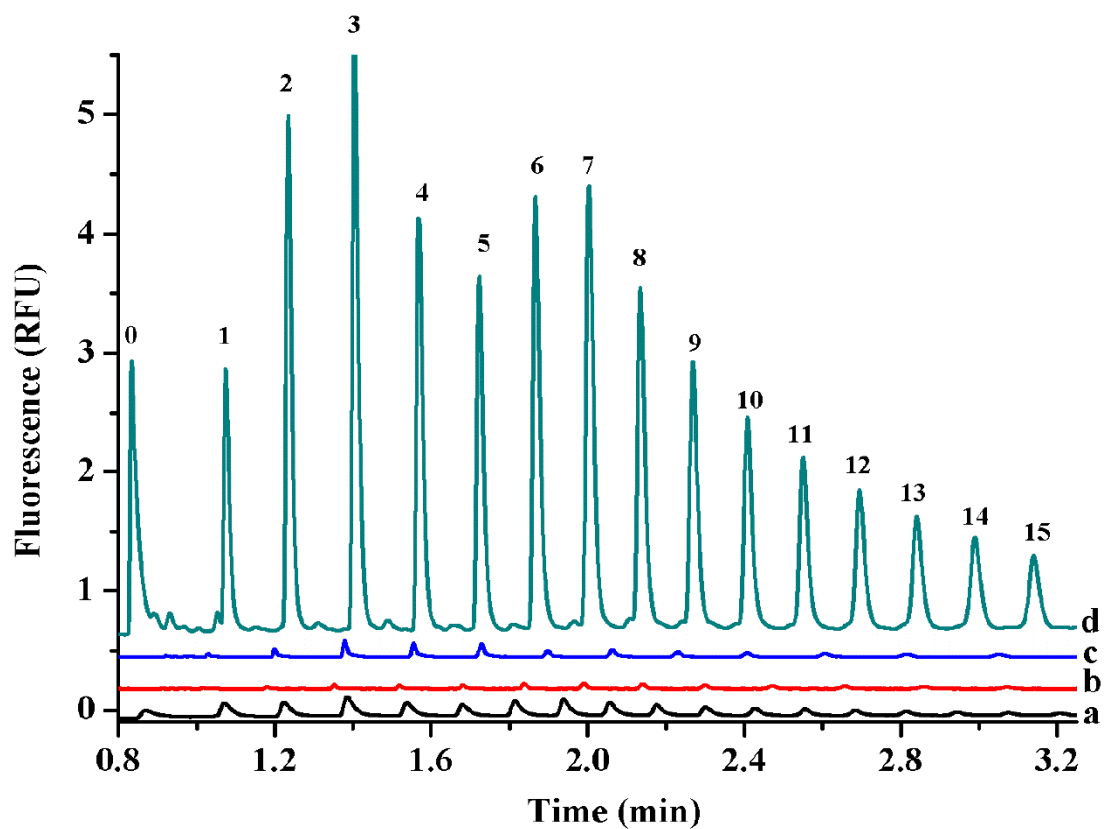
748

749

750

751

752 Fig. 3



753

754

755

756

757

758

759

760

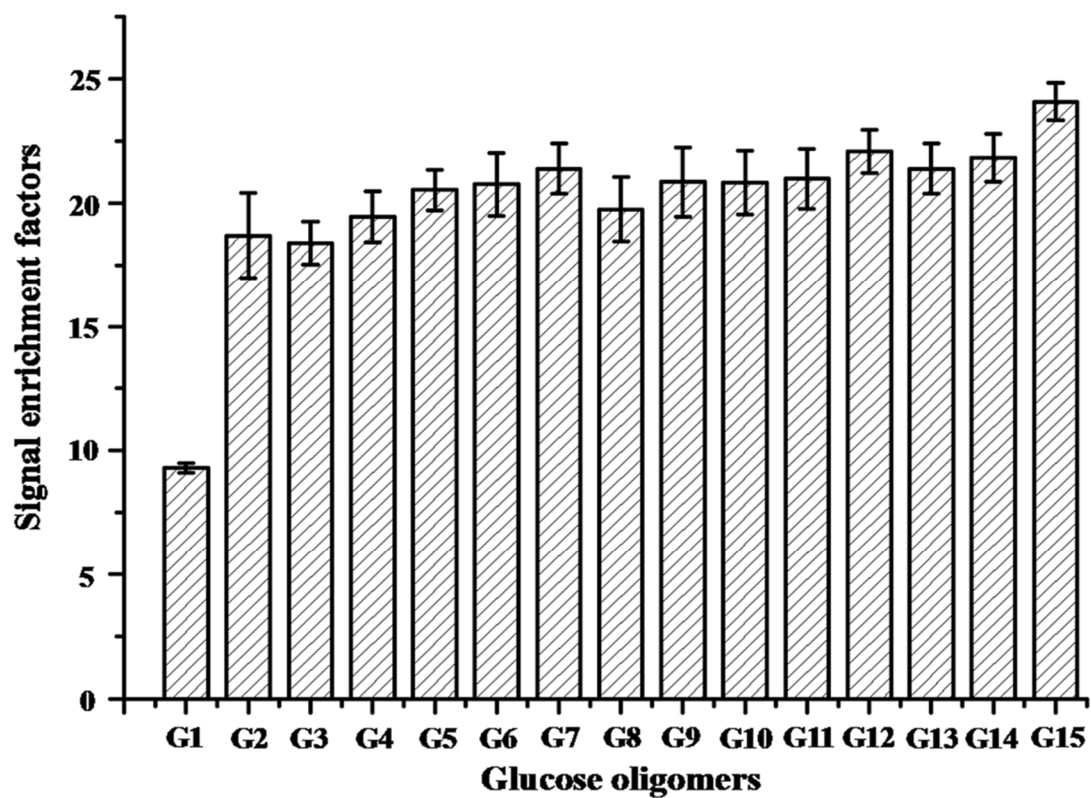
761

762

763

764

765 Fig. 4



766

767

768

769

770

771

772

773

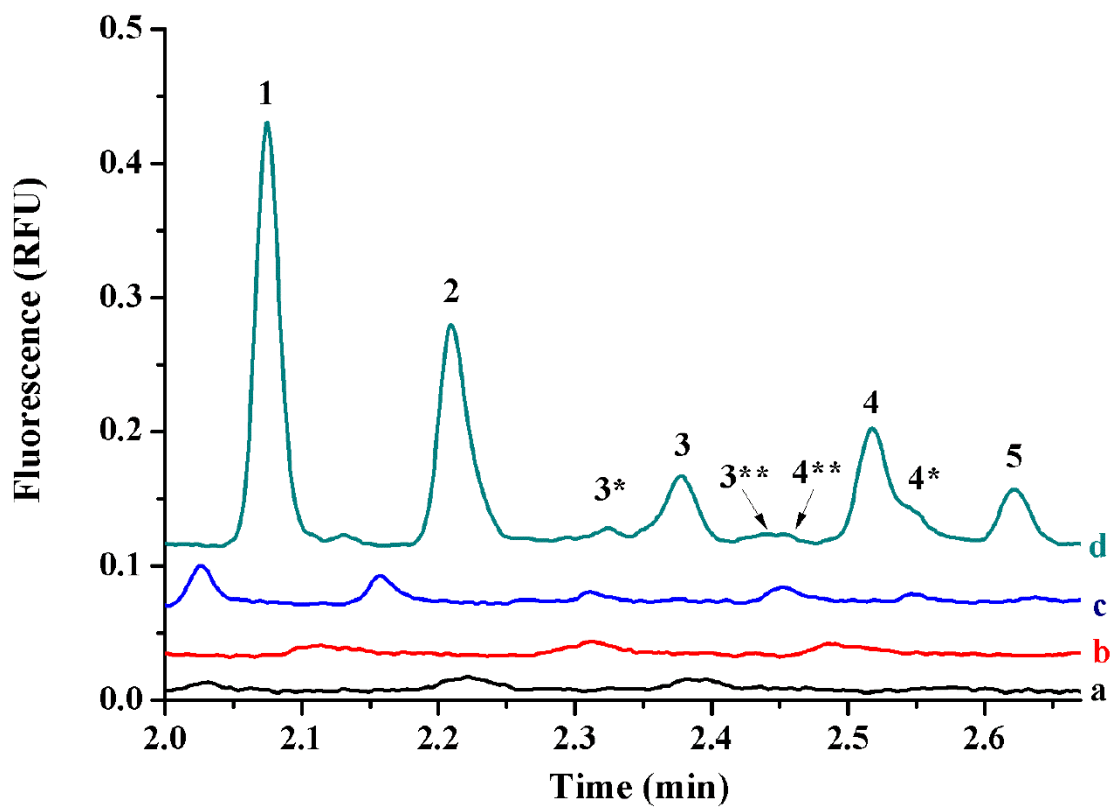
774

775

776

777

778 Fig. 5



779

780

781

782

783

784

785

786

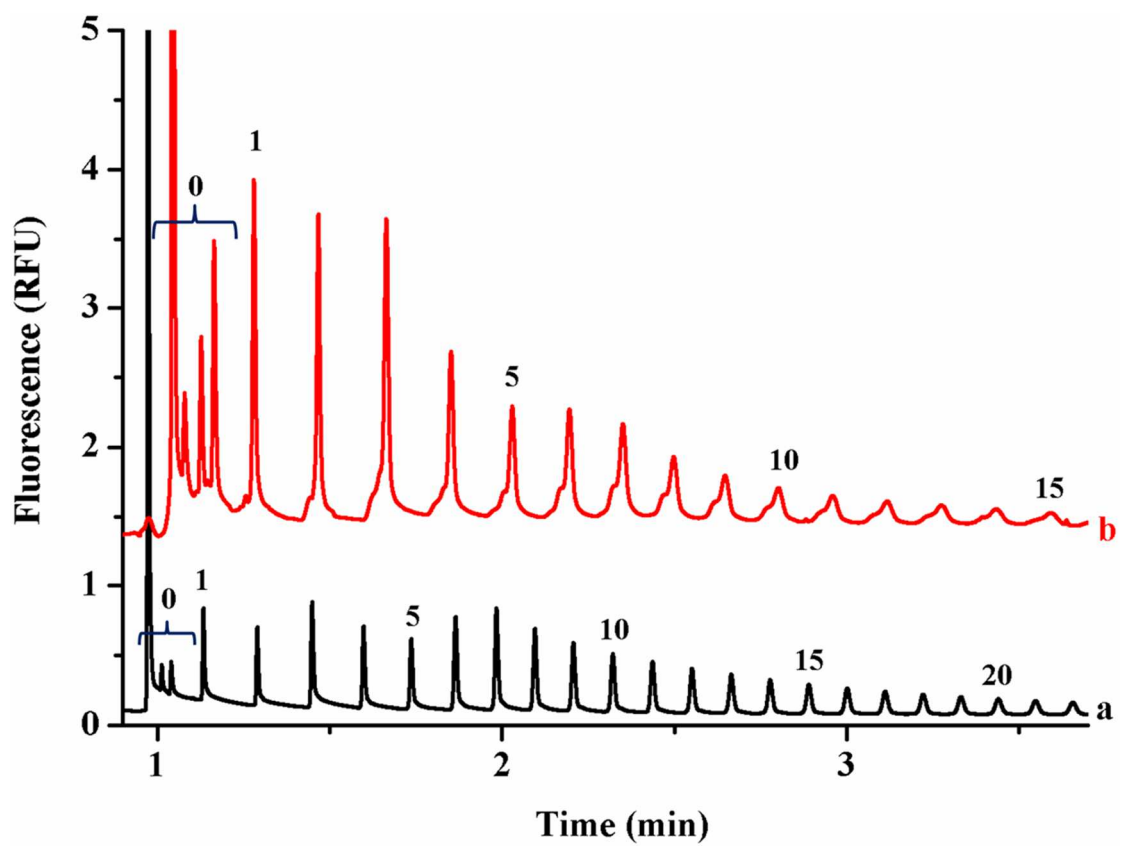
787

788

789

790

791 Fig. 6



792

793

794

795

796

797

798

799

800

801

802

803

804 **Table 1** Permeability of the poly(EGMP-*co*-AM-*co*-BAA) monolith synthesized in a capillary.

Mobile phase	Relative polarity	Viscosity ($\times 10^{-3}$ Pa·s)	Permeability K ($\times 10^{-14}$ m ²)
ACN	0.460	0.369	4.14
MeOH	0.762	0.544	3.85
MeOH/H ₂ O (50/50)	/	1.540	6.12
H ₂ O	1.000	0.890	4.77

805

806

807

808

809

810

811

812

813

814

815

816

817

818

819

820

821 **Table 2** Relative peak area of the five RNase B derived N-glycans labeled with APTS after
 822 enrichment using the Zr⁴⁺ modified poly(EGMP-co-AM-co-BAA) monolith and literature values.

Peak	Relative peak area (%)		Relative peak area (%) (Reported in other studies [42-44])
	After enrichment	RSD (n=3, %)	
Man 5	41.3	2.51	38.4-47.2
Man 6	27.0	1.64	28.0-33.6
Man 7	8.1	6.10	7.2-10.5
Man 8	17.3	4.82	8.6-12.4
Man 9	6.3	3.32	5.2-6.0

823

824

825

Graphical abstract:

